Journal of Optoelectronic and Biomedical Materials Vol. 13, No. 4, October-December 2021, p. 193-201

Green synthesis and characterization of zinc oxide nanoparticles using extracts *of Artemisia annua l.* grown in Togo

K. Sesime, M. M. Dzagli*, K. B. R. Afoudji
Laboratoire de Physique des Matériaux et des Composants à Semi-conducteurs (LPMCS), Département de Physique, Université de Lomé, Lomé, Togo

Plant-mediated synthesis of ZnO nanoparticles (ZnONPs) is preferable than the conventional methods with many applications in medicine and biology. *Artemisia annua* is recognized to have antiplasmodial, antimicrobial activities, so the nanoformulation based on its extracts and zinc oxide would be of therapeutic benefit. This study aims to investigate properties of ZnONPs based on *Artemisia annua* leaves and stems extracts and zinc acetate. Spectroscopy techniques, XRD, SEM and Energy Dispersive X-ray Spectroscopy (EDS) were used to investigate the structural and optical properties of the ZnONPs. The characteristic absorption peak was at 375.5 nm and the excitation at 365 nm showed wide spectra in visible (450-700 nm). XRD, SEM and EDS analysis confirmed a pure ZnONPs in wurtzite hexagonal structure with a size of 21.34 - 24.71 nm. These nanoformulations would be multifunctional and are candidate for treatment of malaria, cosmetics and optoelectronic.

(Received November 15, 2021; Accepted December 8, 2021)

Keywords: Green synthesis, *Artemisia annua*, Togo, Zinc oxide nanoparticles

1. Introduction

Nanotechnologies occupy an important place in today's society thanks to their multiple applications in life (medicine, pharmacy, electronics, energy, environment, chemistry, food and agriculture) [1-3]. They play a real role in the biomedical and pharmaceutical fields thanks to the ease of synthesis of nanoparticles with the desired physical and chemical properties [4, 5]. Organic and inorganic nanoparticles have demonstrated antimicrobial and anticancer activities according to the literature [1, 6-8]. Biosynthesis is an eco-sustainable, environmentally friendly technique that is attracting great attention nowadays in the manufacture and study of materials against the use of physical and chemical methods of synthesis. The biosynthesized nanoparticles are obtained by using as a reducing agent a plant extract, obtained either from roots, leaves, flowers, seeds or fruits and have unique and exceptional characteristics. These properties give nanoparticles the possibility of participating in several mechanisms such as antimicrobial activities and other biomedical applications. Several types of nanoparticles are manufactured today depending on size and shape using the types of reducing agents [9, 10]. Indeed, plants are rich in biomolecules and metabolites (proteins, vitamins, coenzymes, phenols, flavonoids and carbohydrates) which have hydroxyl, carbonyl and amine functional groups. They are responsible for the bioreduction of metal ions into nanoparticles as well as their capping for stability and biocompatibility [11, 12]. Silver, gold and other metals are used to synthesize nanoparticles from plant species but their toxicity towards animals and humans is a real challenge in their use in medicine [13-16]. Zinc oxide (ZnO) is an inorganic compound that is often found in crystalline form. ZnO nanoparticle (ZnONPs) crystalline powder is white with low toxicity and size and shape dependent properties. ZnONPs have been used for applications in textiles, cosmetics, diagnostics, microelectronics and optoelectronics and exhibit antimicrobial properties that can treat infectious diseases and animal pests [17].

The synthesis of ZnONPs from medicinal plant extracts has been the subject of several studies which have demonstrated their antimicrobial activity [18]. Studies were carried on plants such as *Cassia auriculata* [19], *Hibiscus rosasinensi* [20], *Azadirachta indica* or neem [21-23],

* Corresponding author: mdzagli@gmail.com

Olea europea [24], *Aloe barbadensis* [25], *Aloe vera* peel [26], *Ocimum tenuiflorum* [17] and *Camellia sinensis* [27] for biomedical applications. These various studies have demonstrated the value of the synthesis of ZnONPs based on medicinal plant extracts in the health industry [28, 29]. Biosynthesized ZnONPs are considered non-toxic and biocompatible for biomedical applications such as drug carriers, cosmetics, etc. [30]. The present study concerns ZnONPs biosynthesized from plant extracts (*Artemisia annua L.)* used as a bio-reducer. *Artemisia annua L.* is known for its medical value and the extracts from its leaves are believed to have organic molecules that have antioxidant activities to help reducing zinc to nanoparticles [31, 32].

The *Artemisia annua* plant is a highly fragrant, alternate-leaved annual herb of the Asteraceae (Compositeae) family that stands between 30 to 150 centimeters tall. Its taxonomy is defined as follows by Adjogblé et *al.* [33] like: Kingdom: Plantae, Branch: Angiosperms, Class: Dicotyledons, Subclass: Campanulidae, Order: Asteral, Family: Asteraceae, Species: Annua L. It is native from China but its cultivation is done in tropical countries as well as Togo. The use of this plant in traditional medicine has been for centuries and the plant is used in the treatment of malaria and other parasitic diseases. Its leaves are used in herbal medicine and in the pharmaceutical industry because they contain phyto-constituents responsible for numerous pharmacological activities against *Plasmodiums spp* [34], *leishmanias* and cancerous tumors [35, 36].

Thus, in the present study, the objective is to investigate the biosynthesized ZnONPs based on *Artemisia annua* leaves and stems as reducing agents and zinc acetate as a precursor by different techniques for their potential applications. UV–Visible and Fluorescence spectroscopies, X-Ray Diffraction, Scanning Electron Microscopy, Energy-Dispersive X-ray analysis technics were used to perform the properties of the synthesized ZnONPs.

These results will give the characteristics of the ZnO*@Artemisia* complexes and will strengthen their potential use in the biomedical industry.

2. Material and methods

2.1. Chemical and instrumental

Extra pure salt of Zinc acetate dihydrate ($Zn(CH_3COO)_2.2H_2O$) was purchased from DEAJUNG CHEMICALS & METALS Co. LTD, Korea (N^o 8596-4405, CAS N^o 5970-45-6). All chemicals in this experiment were of analytical grade. A solution of zinc acetate ($Zn(CH_3COO)_2.2H_2O$) with a concentration of $1mol.L^{-1}$ is obtained by dissolving 219.5 g of solid zinc acetate in one liter of distilled water with continuous magnetic stirring. A $2\ mol.L^{-1}$ concentration of sodium hydroxide (NaOH) solution was prepared by dissolving 80 g of sodium hydroxide tablets in one liter of distilled water.

The materials used are:

— Magnetic stirrer coupled with a hot plate (0°C-310°C), pHmeter (CHAUVIN ARNOUX Group / PSD1 pH METER), Centrifuge (Biobase), Whatmann filter paper, an oven and glassware (beakers, burette, Erlenmeyer flasks, a graduated cylinder), BUCHI Rotavapor R-100 fitted with a B-100 water bath heating to 40 °C, coupled to a vacuum pump V-100, UV/VIS-Spectrophotometer (UV-5200PC, SHANGHAI METASH INSTRUMENTS, Co.LTD) at the Department of Chemistry of the University of Lomé.

— The SILVA NOVA (StellarNet, USA) spectrometer were used at LPMCS.

— A Siemens D5005 X-ray Diffractometer, with Cu for cathode at wavelength 1.5406*Å* was used at the Laboratory of Crystallography and Molecular Physics, University Felix Houphouet Boigny, Abidjan, Côte d'Ivoire.

— The surface analysis was done on a JEOL JSM-6010plus/LA Analytical Electron Microscope of Elizabeth City State University (North Carolina, USA) using Electron Dispersive X-ray spectroscopy (EDS) to determine the composition of the material.

2.2. Collection of plant material

The stems and leaves, cut and dried, of *Artemisia annua* are purchased from the Sisters Hospitallers NDC at the Divine Misericode farm in Bakakopé (6°39'00.0 "N; 0°54'00.0" E), Municipality of Agou2 (Prefecture of Agou, Plateaux Region, Togo). Bakakopé is located 7 km from Amoussoukopé with is about 75 km from Lomé on the National Road N5. The products are stored at room temperature in the laboratory before being transformed into powder thanks to the electric mill for future use.

2.3. Preparation of the Artemisia annua extract by maceration

The extracts of *Artemisia annua* were prepared by maceration using ethanol and a hydroalcoholic solution (water (V)/ethanol (4V)), respectively. A sample (100 g) of *Artemisia annua* powder is introduced in each solvent and the maceration was carried out gradually. First, 500 mL of each solvent are added to each 100 g of powder in a bottle and the mixture is stirred well regularly. After 24 hours, the contents of the bottle are filtered using Whattman n^{o} 1 filter paper. The filtrate obtained is stored in a flask. Then 500 ml of each solvent are added to the residue obtained during the first 24 hours of filtration and proceed as previously. This is repeated three times for each solvent. The filtrates obtained are subjected to evaporation to remove the solvent using BUCHI Rotavapor. The collected extracts are stored in the refrigerator at 4°C for characterization and future exploitation.

2.4. Green synthesis of ZnONPs

The two ethanolic and hydroethanolic extracts of Artemisia (500 mg) are introduced into 100 mL of their respective solvent to obtain a concentration equal to 5 mg.mL^{-1}. The final solution was successively diluted four times to obtain the five concentrations of 5 mg.mL^{-1}, 3 mg.mL^{-1}, 2 mg.mL^{-1}, 1 mg.mL^{-1} and 0.5 mg.mL^{-1} for the biosynthesis. 50 mL of a zinc acetate solution (1 mol.L^{-1}) are added to 5 mL of each type of *Artemisia* extract of concentration previously defined in a beaker. The mixture of yellowish color with an average pH equal to 5.46 is stirred at 400 rpm at room temperature for approximately 2 hours. Then, a 2 mol.L^{-1} NaOH solution is added drop by drop to reach pH = 11. The mixture is then stirred rigorously at 1000 rpm for more than one hour. A white precipitate forms at the bottom of the beaker. The supernatant was decanted. The white product is washed several times with deionized water to remove impurities and then centrifuged at 2000 rpm for 10 minutes. After centrifugation, the white precipitate is collected, filtered through Whatman n^{o}1 paper and then dried in a vacuum oven at 60 °C. A white powder of ZnONPs is then obtained which is calcined in an oven at 400 °C for 1 hour for future use.

2.5. Characterization of ZnONPs

The synthesized ZnO powders are subjected to different characterization techniques to collect optical information, crystal structure and particle sizes. Optical properties of the synthesized ZnONPs were investigated using UV-VIS - Spectrophotometer (UV-5200PC, 190 - 1100 nm) with a quartz cuvette of 1 cm optical path. ZnONPs powders were dispersed in distilled water and NaOH, respectively for the measurements. Fluorescence spectroscopy was performed on ZnONPs using the SILVA NOVA spectrophotometer. The dissolved samples are excited with a LED of wavelength $\boldsymbol{\lambda}$ = 365 nm. The identification of ZnONPs and its structural phase were performed using a Siemens D5005 X-ray Diffractometer in the range of 2θ=10 °–90 °, with Cu for cathode at wavelength 0.15406 nm. The average size of the ZnONPs was estimated using XRD Crystallite (grain) Size Calculator [37] from the Scherrer formula,

$$D = K\lambda/\beta\cos\theta \quad (1)$$

Where D is the average particle size in nm, λ is the wavelength of the X-ray (nm), β is full width at half maximum (radians) of the diffraction peak, K is the Scherrer constant set at 0.94 [38] and θ is the Bragg angle (radians).

The surface morphology of ZnONPs was investigated using JEOL JSM-6010plus/LA Analytical Electron Microscope and the chemical composition was analyzed by energy dispersive

X-ray spectroscopy (EDS). The ZnONPs were spread on a carbon tape so that it could be held under microscope and also to provide a conductive path.

3. Results and discussions

3.1. UV-Visible analysis

UV-Visible spectroscopy were carried out on biosynthesized ZnONPs in the range from 190-600 nm. Spectra of biosynthesized ZnONPs from different plant extract concentration (a- 5 mg/L, B- 3 mg/L, c- 1 mg/L) of hydroethanolic extracts and ethanolic (A-1 mg/L) were presented on the fig.1. The biosynthesized ZnONPs spectra exhibited absorbance peak at 375.5 nm that confirmed their nanoscale size and it shifted to higher wavelength for ZnONPs base on small concentration of plant extract (Fig.1 - inset). ZnONPs from lower concentration of plant extract spectrum showed an absorbance at 380.5 nm [39, 40].

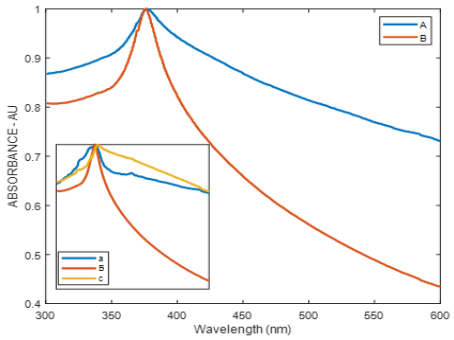

Fig. 1. Normalized absorption spectra of ZnONPs with Hydroethanolic extrats (a-5 mgL^{-1}, B-3 mgL^{-1}, c-1 mgL^{-1}) and Ethanolic extract (A-1 mgL^{-1}) of Artemisia annua.

The energy deviation, obtained from the equation (2):

$$Eg = 1239.83 / \lambda \quad (2)$$

where Eg is the energy of the band expressed in eV and λ (nm) is the maximum absorbance wavelength, was found 3.29 eV.

3.2. Fluorescence spectroscopy

The Normalized fluorescence spectra of the ZnONPs in distilled water and NaOH at an excitation wavelength of 365 nm is shown in fig. 2 for different samples. Fluorescence spectra of synthesized ZnONPs showed wide, very stable and strong emission band of visible range (450-700 nm) from blue to red emission and centred at 557 nm and 550 nm for sample dissolved in distilled water and NaOH, respectively. These results would correspond to the emission due to zinc and oxygen vacancies and the energy gap between the interstitials [41].

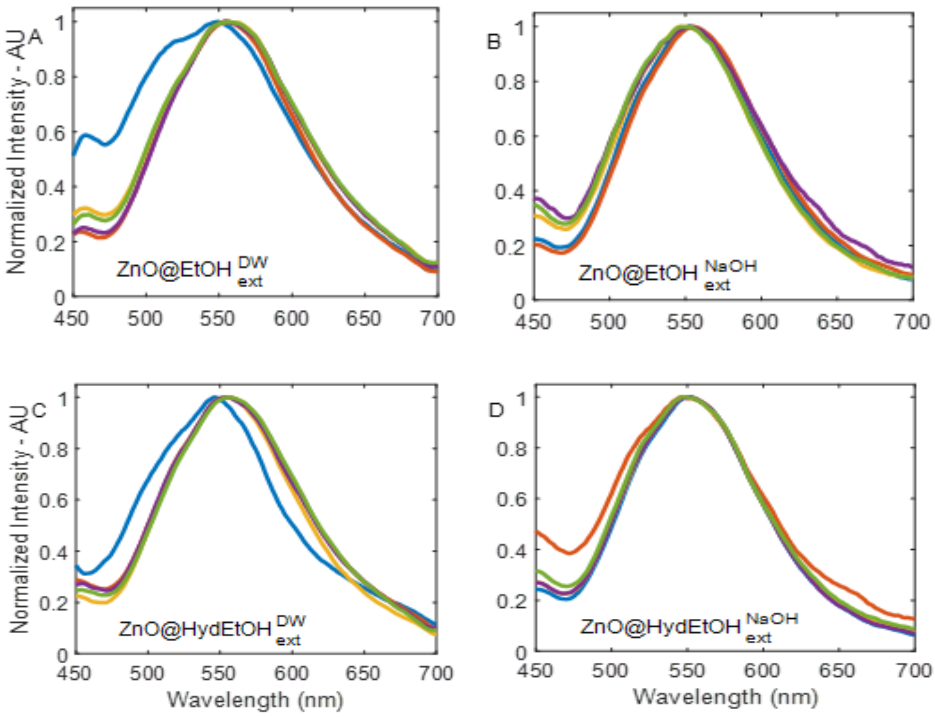

Fig. 2. The Normalized fluorescence spectra of ZnO nanoparticles with (A, B)-Ethanolic and (C, D) -Hydroethanolic extrats of Artemisia annua (0.5mgL^{-1}, 1mgL^{-1}, 2mgL^{-1}, 3mgL^{-1}, 5mgL^{-1})

3.3. XRD analysis

The size of particles and crystallinity of the samples were performed by using XRD analysis. The fig. 3 presents the XRD patterns of the ZnONPs. The sharp diffraction peaks were indexed as (100), (002), (101), (102), (110), (103), (200), (112) and (201) where the two strong peaks correspond to (100) and (101). The ZnONPs Bragg's reflections peaks were found at 2θ value of 31.70, 34.38, 36.22, 47.5, 56.58, 62.82, 66.38, 67.96, 69.04, respectively. The narrow and sharp peaks from the patterns confirmed the well crystalline nature of the biosynthesized ZnONPs. The intense peak in direction (101) confirmed the hexagonal wurtzite phase of the biosynthesized ZnONPs.

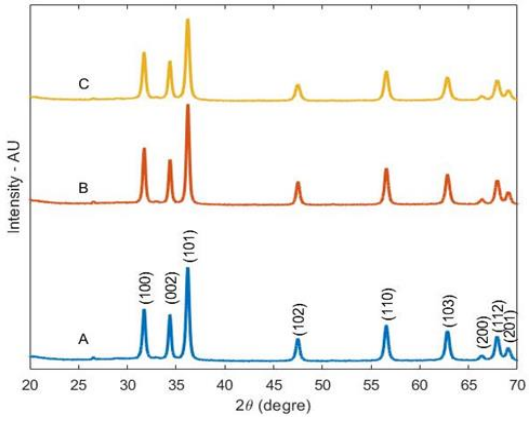

Fig. 3. XRD pattern of ZnO nanoparticles with Hydroethanolic extrats of Artemisia annua (A-@1 mgL^{-1}, B-@3 mgL^{-1}, C-@5 mgL^{-1}).

These findings are in agreement with the results that confirmed the crystalline nature of nanoparticles reporting a similar kind of peak indices for ZnONPs synthesized using different

extracts of *Cassia fistula* and *Melia azadarach* [42], *Calotropis gigantean* [43], *Fungus (Aspargillus niger)* [44], *Scadoxus multiflorus* [45], *Cymodocea serrulata* [46], *L. nobilis* [40], *P. hysterophorus L.* [47], *Nyctanthes arbor-tristis* [48] and green crops [49]. The average size of the ZnONPs was estimated using XRD Crystallite (grain) Size Calculator [37] from the Scherrer formula. XRD analysis revealed the average size (nm) for the three samples from hydroethanolic extrats of *Artemisia annua* (A-@1 mgL^{-1}, B-@3 mgL^{-1}, C-@5 mgL^{-1}) as 21.34, 24.00 and 24.71, respectively. The particle average sizes obtained for the synthesized ZnONPs were in agreement with the previous findings [50].

3.4. SEM-EDS analysis

Scanning electron microscopic images confirmed the surface morphology of zinc oxide nanoparticles (Fig.4.A, Fig.5.A). Agglomerated ZnO nanoparticles were found in clusters with rough surface. Spherical shaped can be observed for the biosynthezed ZnONPs (Fig.4.A) as reported for *Eichhornia crassipes* leaf extract [51], *H. rosa-sinensis* [52], *Calotropis gigantean* [53] and *Zingiber officinale* [54].

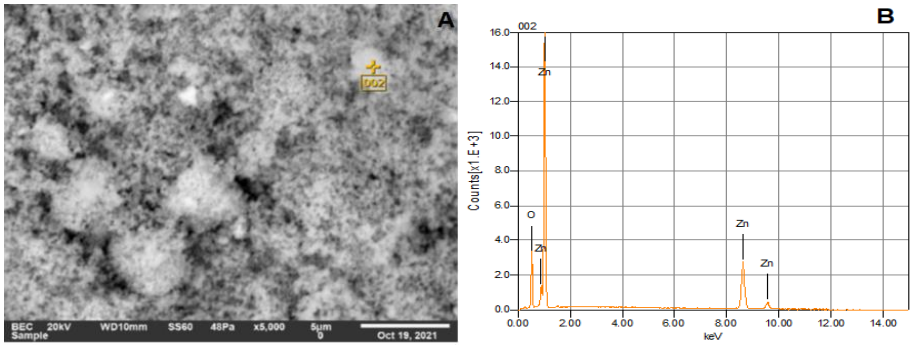

Fig. 4. A- SEM Image of agglomerated, B- EDS spectrum of ZnONPs @Ethanolic extract of Artemisia annua.

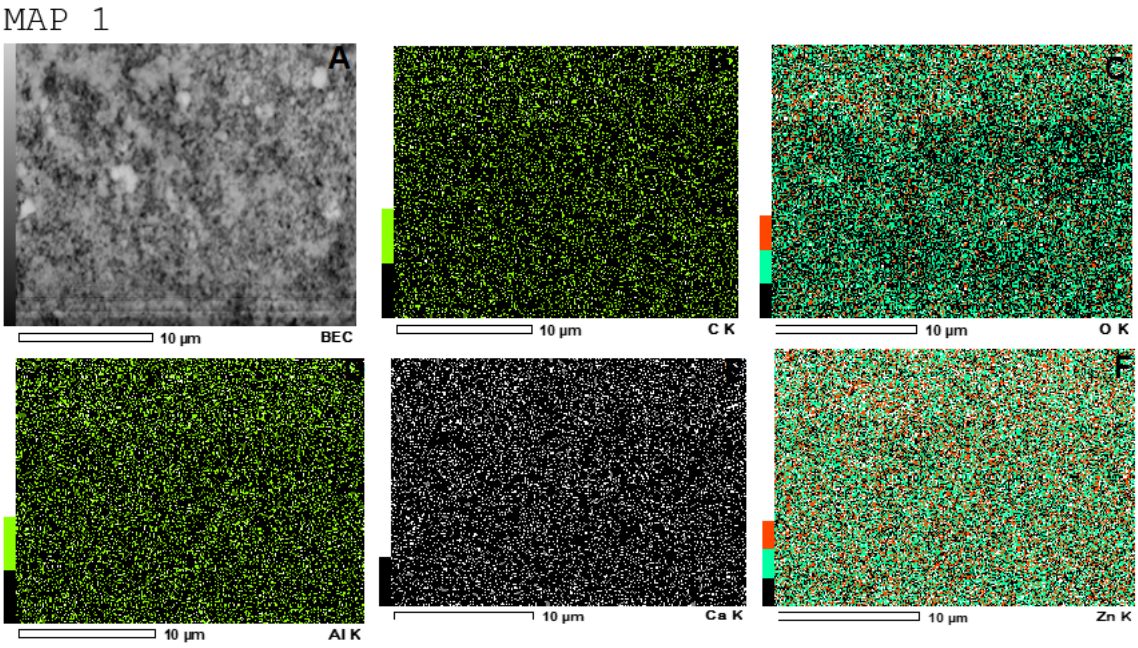

Fig. 5. SEM image of agglomerated ZnONPs @ Hydroethanolic extract with trace elements maps.

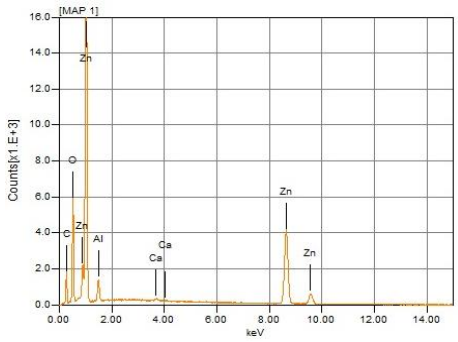

Fig. 6. EDS spectrum of ZnONPs @ Hydroethanolic extrats of Artemisia annua.

The Energy Dispersive X-ray spectrometry (EDS) analysis confirmed the formation of pure ZnONPs from the biosynthesis based on ethanolic extraction with the elements Zn and O (Fig.4.B). The Zn content was 79.23% while O content was 20.77%. The EDS results indicated that ZnONPs were pure and traces of impurities concerning ZnONPs from the biosynthesis based on hydroethanolic extraction with the elements (%) Zn (18.66) and O (33.01), C (46.49), Al (1.74) and Ca (0.11) can be observed on the Fig. 6.

The carbon peak observed could result from some carbon deposition during the calcination of the ZnONPs [50]. The purity, elemental composition and stoichiometry of the synthesized ZnONPs were performed by using EDS analysis. The fig.5 and Fig.6 indicate single peaks of Zn and O between 0 and 2 keV, and the two peaks of zinc between 8 and 10keV. Similar results were reported concerning the same peak position for biosynthesized ZnONPs using *Calotropis gigantean* [43], *Fungus (Aspargillus niger)* [44], *Scadoxus multiflorus* [45], *Cymodocea serrulata* [46] and *L. nobilis* [40].

4. Conclusion

Biosynthesis of zinc oxide nanoparticles using *Artemisia annua* leaf extract is proven to be efficient and environmentally friendly. The synthesized zinc oxide nanoparticles were characterized using UV-Visible, fluorescence spectroscopies and XRD, SEM and EDS techniques. The synthesized ZnO nanoparticles show an absorption peak at 375.5 nm and it moves towards the visible region due to the extract concentration used. The synthesized ZnO nanoparticles exhibit photoluminescence in the visible region (450-700 nm) and it is observed that no defect state is created in the visible region. The XRD analysis confirms the formation of nanoparticles with a particle average size (nm) of 21.34, 24.00 and 24.71, respectively and in the hexagonal wurtzite phase which is the form with the greatest stability of zinc oxide under ambient conditions.

The structural characterization of the synthesized nanoparticles shows a crystalline structure and the hexagonal wurtzite structure of ZnO does not change despite the use of *Artemisia annua* but a visible redshift is observed. The present work proves that it is a simple and inexpensive method to produce ZnO nanoparticles using a medicinal plant like *Artemisia annua.*

Acknowledgements

The authors are grateful to the Head of Chemistry department (University of Lomé) and colleagues such as Dr NOVIDZRO and Dr SALOUFOU. The authors are grateful to the Swedish International Development Cooperation Agency (Sida) through the International Science Programme (ISP), Uppsala University for financial support. The authors are grateful to the African Spectral Imaging Network (AFSIN).

The authors are grateful to Professor Ayayi Claude Ahyi (Auburn University) and Professor Victor Adetayo Adedeji (Elizabeth City State University) for SEM and EDS measurements. The authors are grateful to Dr Eric ZIKI for the XRD measurements at the Laboratory of Crystallography and Molecular Physics, University Felix Houphouet Boigny, Abidjan, Côte d'Ivoire.

References

[1] J. A. Hernández-Díaz, J. J. Garza-García, A. Zamudio-Ojeda, J. M. León-Morales J. C. López-Velázquez, S. García-Morales, Journal of the Science of Food and Agriculture **101**, 1270 (2021).
[2] K. S. Kavitha, S. Baker, D. Rakshith, H. U. Kavitha, B. P. Harini, S. Satish, International Research Journal of Biological Sciences **2**, 66 (2013).
[3] P. Malik, R. Shankar, V. Malik, N. Sharma, T. K. Mukherjee, Journal of Nanoparticles **2014**, 302429 (2014).
[4] J. R. Heath, PNAS **112**(47), 14436 (2015).
[5] A. Aggarwal, Nanotechnology Letters **1**(1), 5 (2017).
[6] Y. Bao, J. He, K. Song, J. Guo, X. Zhou, S. Liu, Journal of Chemistry **2021**, 6562687 (2021).
[7] K. S. Prasad, S. K. Prasad, M. A. Ansari, M. A. Alzohairy, M. N. Alomary, S. AlYahya, C. Srinivasa, M. Murali, V. M. Ankegowda, C. Shivamallu, Biomolecules **10**(7), 982(2020).
[8] Naveen Priya, K. Kaur, A. K. Sidhu, Frontiers in Nanotechnology **3**, 655062 (2021).
[9] X. Geng, T. Z. Grove, In: Udit A. (eds) Protein Scaffolds. Methods in Molecular Biology, Humana Press, New York, 1798 (2018).
[10] V. N. Kalpana, V. D. Rajeswari, Bioinorganic Chemistry and Applications **2018**, 3569758 (2018).
[11] V. V. Makarov, A. J. Love, O. V. Sinitsyna, S. S. Makarova, I. V. Yaminsky, M. E. Taliansky, N. O. Kalinina, Acta Naturae **6**(1), 35 (2014).
[12] B. Biswas, K. Rogers, F. Mclaughlin, D. Daniels, A. Yadav, International Journal of Microbiology **2013**, 746165 (2013).
[13] A. K. Mittal, Y. Chisti, U. C. Banerjee, Biotechnology Advances **31**(2), 346 (2013).
[14] R. Rajan, K. Chandran, S. L. Harper, S. I. Yun, P. T. Kalaichelvan, Industrial Crops and Products **70**, 356 (2015).
[15] S. Ahmed, M. Ahmad, B. L. Swami, S. Ikram, Journal of Advanced Research **7**, 17 (2016).
[16] S. K. Chandraker, M. K. Ghosh, M. Lal, R. Shukla, Nano Express **2**(2), 022008 (2021).
[17] N. J. Sushma, B. Mahitha, K. Mallikarjuna, P. R. B. Deva, Applied Physics A **122**, 544 (2016).
[18] S. Modi, M. H. Fulekar, Journal of Nanostructures **10**(1), 20 (2020).
[19] P. Ramesh, A. Rajendran, M. Sundaram, Journal of NanoScience and NanoTechnology **2**, 41 (2014).
[20] M. J. Divya, C. Sowmia, K. Joona, K. P. Dhanya, Research Journal of Pharmaceutical, Biological and Chemical Sciences **4**(2), 1137 (2013).
[21] A. Sivalingam, T. Balusamy, S. S. J. Krishnan, P. K. Nagarajan, Biomass Conversion and Biorefinery, https://doi.org/10.1007/s13399-021-01344-w (2021).
[22] S. Suganya, S. Vivekanandhan, Journal of the Australian Ceramic Society **55**, 433 (2019).
[23] C. Abinaya, R. Manjula Devi, P. Suresh, N. Balasubramanian, N. Muthaiya, N. D. Kannan, J. Annaraj, V. Shanmugaiah, J. M. Pearce, P. Shanmugapriya, J. Mayandi, Nano Express **1**(1), 010029 (2020).
[24] A. Awwad, B. Albiss, A. L. Ahmad, Advanced Materials Letters **5**, 520 (2014).
[25] S. Gunalan, R. Sivaraj, V. Rajendran, Progress in Natural Science: Materials International **22**, 693 (2012).
[26] A. Chaudhary, N. Kumar, R. Kumar, R. K. Salar, SN Applied Sciences **1**, 136 (2019).
[27] R. K. Shah, F. Boruah, N. Parween, International Journal of Current Microbiology and Applied Sciences **4**, 444 (2019).
[28] H. Hamrayev, K. Shameli, S. Korpayev, Journal of Research in Nanoscience and

Nanotechnology **1**(1), 62 (2021).
[29] A. Vignesh, S. Selvakumar, K. Vasanth, Nanomedicine Research Journal **6**(2), 128 (2021).
[30] M. Ovais, A. Nadhman, A. T. Khalil, A. Raza, F. Khuda, M. F. Sohail, N. U. Islam, H. S. Sarwar, G. Shahnaz, I. Ahmad, M. Saravanan, Z. K. Shinwari, Nanomedicine (Lond) **12**(24), 2807 (2017).
[31] T. Czechowski, M. A. Rinaldi, M. T. Famodimu, M. Van Veelen, T. R. Larson, T. Winzer, D. A. Rathbone, D. Harvey, P. Horrocks, I. A.Graham, Frontiers in Plant Science **10**, 984 (2019).
[32] B. M. Gruessner, P. J. Weathers, PLoS ONE **16**(3), e0240874 (2021).
[33] M. K. Adjogblé, B. Bakoma, K. Metowogo, K. D. Amouzou, Y. Potchoo, K. Eklugadegbeku, K. A. Aklikokou, M.Gbeassor, Pharmacognosy Journal **11**(6), 1331 (2019).
[34] M. J. Abad, L. M. Bedoya, L. Apaza, P. Bermejo, Molecules **17**(3), 2542 (2012).
[35] M. P. C. Ortiz, M. Q. Wei, Journal of Biomedicine and Biotechnology **2012**, 1 (2012).
[36] B. Koul, P. Taak, A. Kumar, T. Khatri, I. Sanyal, Journal of Glycomics & Lipidomics **7**, 142 (2017).
[37] XRD Crystallite (grain) Size Calculator (Scherrer Equation) – InstaNANO. https://instanano.com/characterization/calculator/xrd/crystallite-size/
[38] H. Irfan, K. Mohamed Racik, S. Anand, Journal of Asian Ceramic Societies **6**(1), 54 (2018).
[39] S. Nagarajan, K. Arumugam Kuppusamy, Journal of Nanobiotechnology **11**, 39 (2013).
[40] S. Fakhari, M. Jamzad, H. Kabiri Fard, Green Chemistry Letters and Reviews **12**(1), 19 (2019).
[41] Udayabhanu, G. Nagaraju, H. Nagabhushana, D. Suresh, C. Anupama, G. K. Raghu, S. C. Sharma, Ceramics International **43**(15), 11656 (2017).
[42] M. Naseer, U. Aslam, B. Khalid, B. Chen, Scientific Reports **10**, 9055 (2020).
[43] S. K. Chaudhuri, L. Malodia, Applied Nanoscience **7**(8), 501 (2017).
[44] A. Shamim, T. Mahmood, M. B. Abid, International Journal of Chemistry **11**, 119 (2019).
[45] N. Al-Dhabi, A. M. Valan, Nanomaterials **8**(7), 500 (2018).
[46] S. Rajeswaran, S. Somasundaram Thirugnanasambandan, S. Rengasamy Subramaniyan, S. Kandasamy, R. Vilwanathan, Applied Physics A **125**, 105 (2019).
[47] P. Rajiv, S. Rajeshwari, R. Venckatesh, Spectrochimica Acta Part A: Molecular and Biomolecular Spectroscopy **112**, 384 (2013).
[48] P. Jamdagni, P. Khatri, J. S. Rana, Journal of King Saud University – Science **30**(2), 168 (2018).
[49] N. Jayarambabu, B. Siva Kumari, K. Venkateswara Rao, Y. T. Prabhu, International Journal of Multidisciplinary Advanced Research Trends **II**(I), 273 (2015).
[50] M. R. Kamli, M. A. Malik, V. Srivastava, J. S. M. Sabir, E. H. Mattar, A. Ahmad, Pharmaceutics **13**, 1743 (2021).
[51] P. Vanathi, P. Rajiv, S. Narendhran, S. Rajeshwari, P. K. S. M. Rahman, R. Venckatesh, Materials Letters **134**, 13 (2014).
[52] M. J. Divya, C. Sowmia, K. Joona, K. P. Dhanya, Research Journal of Pharmaceutical, Biological and Chemical Sciences **4**, 1137 (2013).
[53] K. Subham, J. Kaur, M. Chakroborty, S. G. A. Manuel, N. Pradeep, Journal of Advanced Scientific Research **11**(3), 183 (2020).
[54] L. F. A. Anand Raj, E. Jayalakshmy, International Journal of Pharmacy and Pharmaceutical Sciences **7**, 384 (2015).